Performance Assessment of an Air-to-Air Heat Pump with Advanced Technologies Based on Exergy Analysis

Goran Vučković[a], Mirko Stojiljković[b], Marko Ignjatović[c] and Mića Vukić[d]

[a] *University of Niš, Faculty of Mechanical Engineering in Niš, Serbia, goran.vuckovic@masfak.ni.ac.rs, CA*
[b] *University of Niš, Faculty of Mechanical Engineering in Niš, Serbia, mirko.stojiljkovic@masfak.ni.ac.rs*
[c] *University of Niš, Faculty of Mechanical Engineering in Niš, Serbia, marko.ignjatovic@masfak.ni.ac.rs*
[d] *University of Niš, Faculty of Mechanical Engineering in Niš, Serbia, mica.vukic@masfak.ni.ac.rs*

Abstract. The buildings sector has a significant impact on the environment, considering that in addition to industry and transport among the largest consumers of energy. Preservation of the external appearance of building facades and high standards in terms of thermal comfort have led to the development of systems in which many indoor units can be connected to a single outdoor unit. Such systems are widely known as VRV/VRF (Variable Refrigerant Volume/Variable Refrigerant Flow) systems. However, the constant need to increase energy efficiency has given rise to new technology, named VRT (Variable Refrigerant Temperature). Here, the first and second law approach of an air-source heat pump with modern control strategies which worked in the moderate continental climate was performed. To fully understand the processes, the total exergy destruction for every main component split unavoidable and avoidable part. The results show the biggest negative impact on exergy efficiency of observed system has internal ireversibilities in the speed control compressor with 17.4%. Destroyed work in other main components generated cumulative negative impact of 26.7% and the exergy losses reduced exergy efficiency by 33.5%. If the available modern technologies are applied, the 27% of destroyed useful work in compressor can be avoided, but the bigger part (73%) is unavoidable.

Keywords: Heat pump, exergy analysis, VRV&VRT.

Email: Goran Vučković <goran.vuckovic71@gmail.com>

1. Introduction

The sales of heat pumps worldwide decreased by 3% in 2023 compared to the previous two years when the market recorded double-digit growth [1]. In the Europe in the first half of 2024 the heat pump sales decrease by 47% compared to the same period in 2023 [2]. Changing national policies and measures of subsidies are cited as a key reason for the slowdown in heat pump sales. Consumers are extra restrained, especially in conditions of inflation and high interest rates, because the investment in heat pumps generally is high [1,2]. From the other hand, the implementation of advanced modern technologies in heat pump sector (for example, Internet of Things - IoT and Artificial Intelligence - AI) and rising investments in development and research, have a positive impact on even greater representation of heat pumps worldwide [3].

The development of air-to-air heat pumps or air-source heat pumps (ASHP) represent a turning point to implementing energy sustainable technologies. During the more than half century long history ASHPs are permanently improved and today represent a leading technology for heating and cooling worldwide. The inverter technology allows ASHPs to adjust working frequency of compressor and capacity output of heat pump based on heating and cooling demand [4].

The VRV/VRF technology as a next level of inverter technology. That term refers to the ability of the system to manage the amount of refrigerant that flows through the heat exchanger, and in this way, the capacity of the heat exchanger can be changed in each individual space, i.e. individually adjustable comfort level. Additional improvements are reflected in the implementation novel VRV system control strategy named and VRT, which further increases the system efficiency and contributes to reducing wear of the main heat pump components. The variable refrigerant evaporating temperature in the cooling regime and the variable refrigerant condensing temperature in the heating regime, represents in general VRT strategy or technology. Also, VRV and VRT technologies are compatible with independent indoor temperature control in different spaces, in case when using the same system for simultaneous cooling and heating in different part of building, known as "three-pipe system", VRV heat recovery system (VRV-HR) or multifunctional system.

The VRF as one of up-to-date technology in the thermal comfort of building sector, has been implemented for decades at first in Asia, also in Europe, but not less on the North America market [5]. The scientists and manufacturers have been making constant efforts to improve performance of ASHP with VRF technology, with develop new advanced functions. Some research focus on integrated operation with other systems, other to the introduction of better design of components, and some of them to enhanced control logics [6]. Authors in [7] shown a new approach of the VRF heat pump with the integrated dehumidification operations and a self-regenerating heat pump draying unit. The variable refrigerant temperature (VRT) technique is one very important and successful example, which can modulation temperature of refrigerant at various operational conditions together with the dynamic change of the flow rate. The VRT technology evaluates the heating or cooling load conditions of all the spaces served by the energy system and dynamic regulate temperature (condensation or evaporation) of refrigerant for better system performance [8].

In paper [9] for the VRF system worked in cooling regime, was developed a refrigerant evaporating temperature control algorithm or VRT control algorithm. The effects were tested in actual buildings and verified through an experimental investigation. The needs for dehumidification of indoor units decreases when the evaporation temperature increases from 8 to 12 Celsius degrees. The electricity consumption decreased by 16.8% for the education building and 13.5% for the office building.

Authors in the paper [10] for five office buildings constructed in different periods in Greece (Thessaloniki and Athens) evaluated the relationship between the life cycle cost (LCC) and primary energy consumption (PEC) including used of VRV technology. The results shown that for all buildings (regardless of climate zones or construction periods) and the VRV technology is lead to the lowest LCC and PEC. The general conclusion was that the VRV technology is a very useful for ultra-low energy buildings (nearly zero energy building - nZEB) and most cost-effectively buildings.

In paper [11] researchers have examined VRF system which can simultaneously provide heating and cooling of spaces and heating of sanitary water. The goal was to research the impacts on energy performance of a multifunctional VRF system during the cooling and heating periods, in the building with high values of internal heat sources. The multifunctional VRF system have the great potential for energy saving in summer period and small potential in the low heating load in the winter period. The results were verified during the performance test.

The paper [12] provided experimental and theoretical approach of additional control strategy (named VRT) under the part load conditions in the summer period, for an existing VRV system. In the smaller load (especially lower than 50%) the VRT control technique have a positive impact to reduce consumption of energy. The review paper [13] offered a detailed overview of multi-split VRF systems. The overview consists analyses of the applications, operations, configurations, cost comparison and marketing aspects.

In this paper authors using theoretical analysis based on first and second laws investigates efficiency of ASHP with simultaneous VRV&VRT techniques in heating regime under the part load conditions. It was applied the energy and exergy approach for verified by experimental results. The results confirmed that the simultaneous VRV&VRT techniques can help to reduce consumption of energy in observed conditions.

2. Heat pump description and procedure of measurement

The observed system has an outdoor unit and many indoor units in offices (13 units in total), every indoor unit with direct expansion, figure 1. The refrigerant is R410A. In the outdoor unit, the main components are compressor (CM), four-way reversing valve, a finned tube heat exchanger (EV) (evaporator in heating operation mode) with axial propeller fan and expansion valve (EEV). Detailed parameters of outdoor and indoor units presented in table 1.

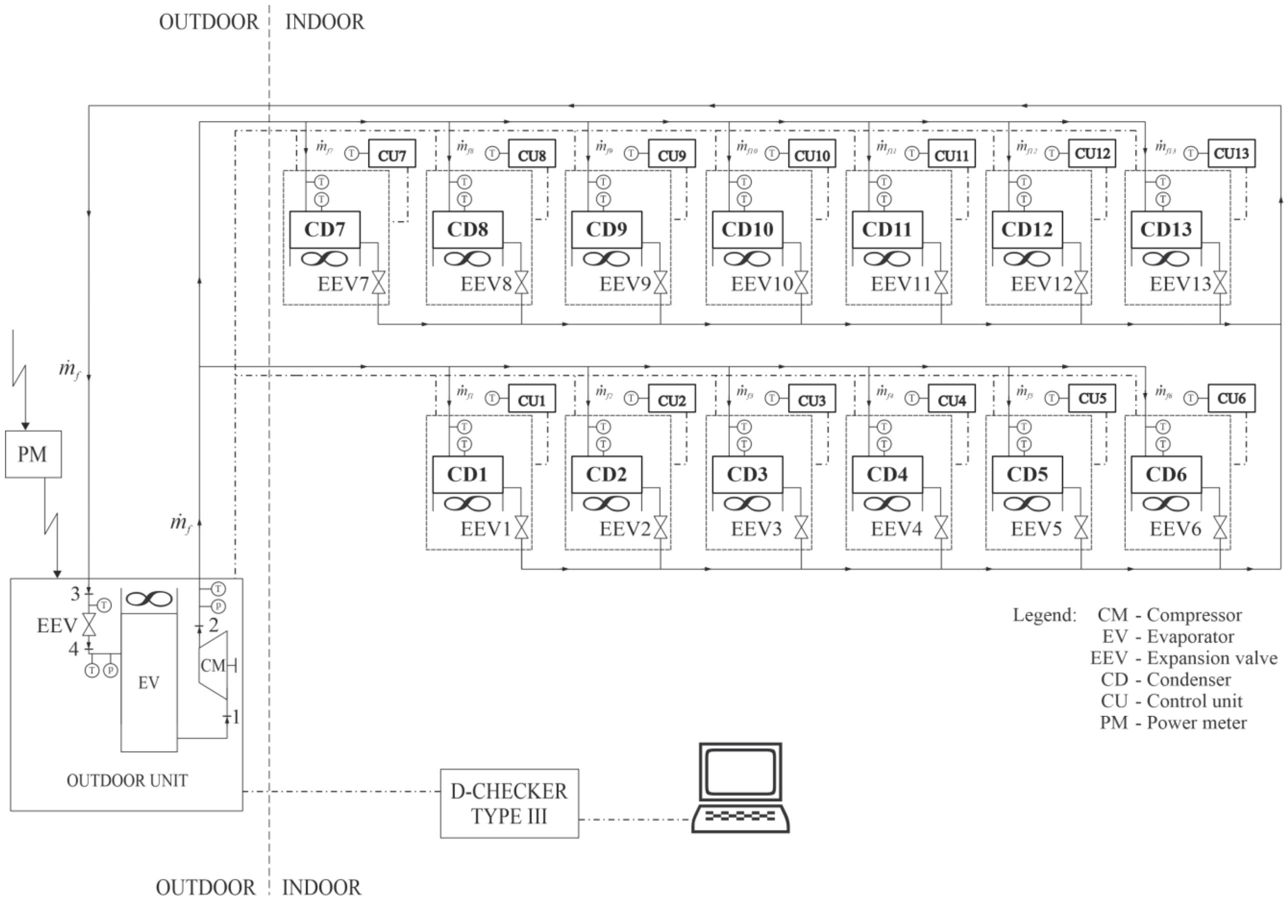

Figure 1. Schematic of the ASHP with VRV&VRT control techniques

In this research the four-way reversing valve was in position for heating mode (heat pump regime). The VRV technology changing the refrigerant flow rate with changing the compressor operation frequency, depending on the heating needs of the spaces. The heat pump efficiency increases when the compressor frequency reduced, figure 2c.

Table 1. Parameters of outdoor and indoor units [14]

Heat pump unit	Model	Quantity	Capacity [kW]		Power input [kW]	
			Heating	Cooling	Heating	Cooling
Outdoor	RXYQ10P7W1B	1 piece	31.5	28.0	7.70	7.42

Indoor	FXDQ20M8V3B	11 pieces	2.5	2.2	0.05	0.05
Indoor	FXCQ25M8V3B	1 piece	3.2	2.8	0.059	0.092
Indoor	FXFQ25P7VEB	1 piece	3.2	2.8	0.045	0.053

Three different models were used for the indoor units, but essentially with the same components: an electronic expansion valve (EEVm) and finned tube heat exchanger (CDm) (condenser) with the fan, figure 1. The EEVm permanently adapts flow rate of refrigerant in accordance with heating needs in offices. Regulation was based on the air temperature in the space measured via temperature sensor in the wall control unit. The role of the fan is to provide forced airflow from the room through the condenser.

In the heating season (winter, cold autumn/spring) the ASHP provides heating effect to the space taking heat energy from the outdoor air through a finned tube air-to-refrigerant heat exchanger. In that period, the heating load of the space get lower when the outdoor temperature gets higher, figure 2a. Every period with partial load that is exactly the situation when the heat pump efficiency increases using VRT technology. The lower load for heating needs the lower refrigerant condensing temperature and lower power input for the compressor operation, and finally better efficiency of the ASHP, figure 2.

The observed energy system (outdoor unit and all indoor units) is connected on the electricity public network via a digital power meter (PM) which registered the power consumption only for the heat pump system. To monitor the outdoor temperature, indoor temperatures and condenser inlet temperatures in offices, T-type thermocouples have been deployed. Also, to monitor discharge, subcooling and evaporating temperatures of refrigerant, Pt-100 type sensors have been mounted on the installation. The pressure sensors registered discharge gas phase and evaporating pressure of refrigerant, figure 1. The wall control unit (CU) used for control operation of each indoor unit.

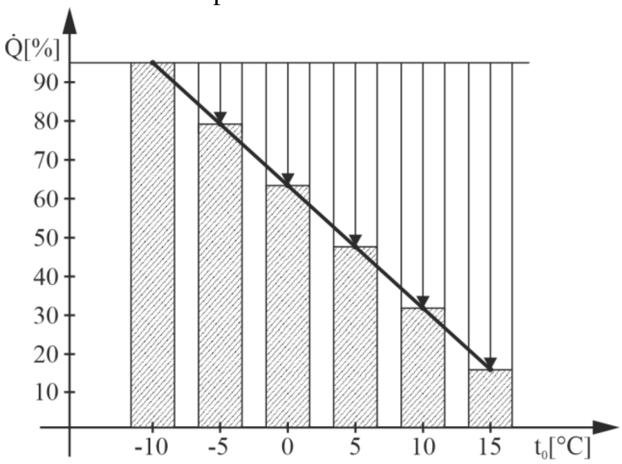

a) Heating load vs outdoor temperature

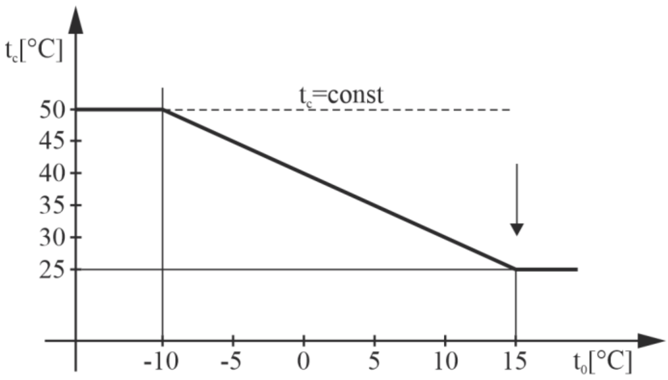

b) Condensing temperature vs outdoor temperature

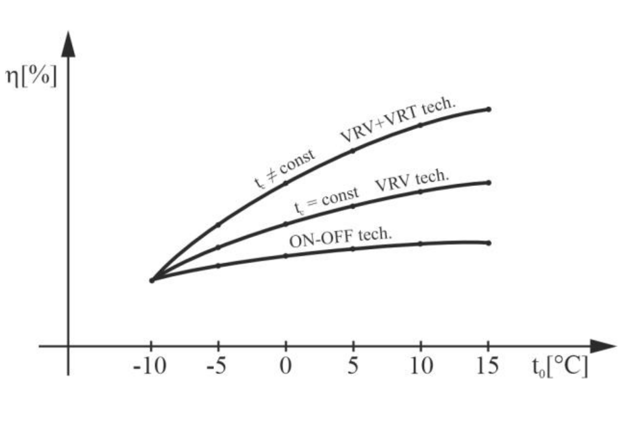

c) Efficiency with different technologies

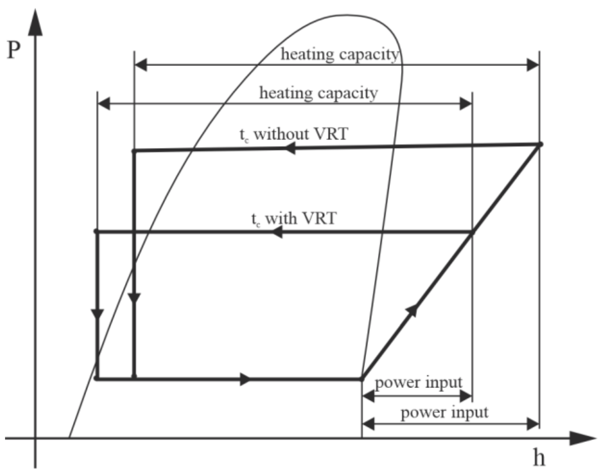

d) VRT impact on power reduction

Figure 2. Positive impacts in partial load

The measurements were implemented in the period from 18:10:00 (07-03-20237) to 05:37:00 (08-03-2023), during which 1,959 readings were recorded for every parameter. The measured values were recorded every 20 seconds. The setpoint of the indoor air temperature as a main control parameter was 26 degree ($t_{u,tar}$ = 26°C).

During the experiment, one indoor unit (number 3) was not functional due to a breakdown. All data were collected using original device from heat pump producer, for monitoring and diagnostics (D-Checker, Type III.1), figure 1. The table 2 provide the summary information about equipment, measuring range and accuracy.

Table 2. Measuring equipment, range and accuracy

Measuring equipment	Measurement range	Accuracy
Digital power meter	5 – 60 A	± 0.5%
T-type thermocouple	-200 – 350°C	± 0.8%
Pt-100 temperature sensors	-80 – 400°C	± 0.8%
Pressure sensors P110	0 – 200 bar	± 1%

For calculating thermal, energy and exergy variables of process fluids were used the measurements value of the different parameters. During the experimental investigation, we collected a large number of measured data for processing fluids (refrigerant, outdoor and indoor air) and data of electricity consumption. The further analysis was based on the basic statistical quantities as standard deviation (STD), median (MED) and average value (AVR). The statistical quantities were determined by using the equations [15]:

$$\sigma_X = \left| \sqrt{\frac{1}{N}\sum_{i=1}^{N}(X_i - \bar{X})^2} \right| \tag{1}$$

$$\mu_X = \begin{cases} X_i, where\ is\ i = (N+1)/2\ and\ N\ odd\ number \\ \dfrac{X_i + X_{i+1}}{2}, where\ is\ i = N/2\ and\ N\ even\ number \end{cases} \tag{2}$$

$$\bar{X} = \frac{1}{N}\sum_{i=1}^{N} X_i \tag{3}$$

3. Evaluation methodology

The maximum efficiency of heat pump is achieved when the heat pump operates with isothermal and isentropic reversible processes (the Carnot cycle). Coefficient of performance of Carnot cycle (COP_C) depends only on two temperatures of reservoirs (heat source reservoir/evaporating temperature and heat sink reservoir/condensing temperature) [16]:

$$\mathrm{COP_{C,tot}} = \mathrm{COP_C} = \frac{T_{\mathrm{con}}}{T_{\mathrm{con}} - T_{\mathrm{evp}}} = \frac{T_{\mathrm{con}}}{\Delta T_{\mathrm{lift}}}. \tag{4}$$

In all real cycles the performance is lower than the performance of ideal Carnot cycle. In accordance with previous the heat pump COP can be expressed by the expression:

$$\mathrm{COP_{tot}} = \frac{\Sigma \dot{Q}_{\mathrm{CD}m}}{\dot{W}_{\mathrm{tot}}} = \frac{\dot{Q}_{\mathrm{tot}}}{\dot{W}_{\mathrm{tot}}}; \qquad (\mathrm{COP_{tot}} < \mathrm{COP_{C,tot}}). \tag{5}$$

In equation (5) the dividend represents the final heat delivered to the indoor spaces (all offices). The delivered heat to each end-user (office) determined as:

$$\dot{Q}_{\mathrm{CD}m} = \dot{m}_{fj}\left(h_{j,\mathrm{e}} - h_{j,\mathrm{i}}\right). \tag{6}$$

Also, in equation (5) the divisor represents the total power input, or sum of the electrical energy input to drive the speed control compressor, all fans in indoor units (condensers), and speed control fan on evaporator, as shown:

$$\dot{W}_{\mathrm{tot}} = \dot{W}_{\mathrm{CM}} + \Sigma\dot{W}_{\mathrm{CD}m} + \dot{W}_{\mathrm{EV}}. \tag{7}$$

However, much better information about the efficiency of the energy system is provided by an analysis based on the second law of thermodynamics. The exergy efficiency of component or of overall system defined as the ratio between the adequate exergy of product and exergy of fuel, in the fuel-product concept [17]:

$$\varepsilon_{\mathrm{k}} = \frac{\dot{E}_{\mathrm{P},k}}{\dot{E}_{\mathrm{F},k}} = 1 - \frac{\dot{E}_{\mathrm{D},k} + \dot{E}_{\mathrm{L},k}}{\dot{E}_{\mathrm{F},k}}; \qquad \varepsilon_{\mathrm{CD}m} = \frac{\dot{E}_{\mathrm{P,CD}m}}{\dot{E}_{\mathrm{F,CD}m}} = 1 - \frac{\dot{E}_{\mathrm{D,CD}m} + \dot{E}_{\mathrm{L,CD}m}}{\dot{E}_{\mathrm{F,CD}m}}. \tag{8}$$

$$\varepsilon_{\mathrm{tot}} = \frac{\Sigma\dot{E}_{\mathrm{P,CD}m}}{\dot{E}_{\mathrm{F,tot}}} = \frac{\dot{E}_{\mathrm{P,tot}}}{\dot{E}_{\mathrm{F,tot}}} = 1 - \frac{\dot{E}_{\mathrm{D,tot}} + \dot{E}_{\mathrm{L,tot}}}{\dot{E}_{\mathrm{F,tot}}}. \tag{9}$$

The previous expressions are based on the exergy balance in component and overall level, as follows:

$$\dot{E}_{\mathrm{F},k} = \dot{E}_{\mathrm{P},k} + \dot{E}_{\mathrm{D},k} + \dot{E}_{\mathrm{L},k}; \quad \dot{E}_{\mathrm{F,CD}m} = \dot{E}_{\mathrm{P,CD}m} + \dot{E}_{\mathrm{D,CD}m} + \dot{E}_{\mathrm{L,CD}m}; \quad \dot{E}_{\mathrm{F,tot}} = \dot{E}_{\mathrm{P,tot}} + \dot{E}_{\mathrm{D,tot}} + \dot{E}_{\mathrm{L,tot}}. \tag{10}$$

It is important to point out that very often the surrounding temperature is taken as the boundary of the system component, and then all irreversibilities destroyed exergy (the component exergy loss equals zero), but there is the total exergy loss.

The exergy destruction of every component of energy system obtained from component exergy balance in the steady state conditions [18]:

$$0 = \sum_j \left(\left(1 - \frac{T_0}{T_j}\right)\dot{Q}_j\right)_k - \dot{W}_{\mathrm{cv},k} + \sum_i (\dot{m}_i e_i)_k - \sum_e (\dot{m}_e e_e)_k - \dot{E}_{\mathrm{D},k}. \tag{11}$$

The standard conditions for pressure (p_0=1.01325 bar) and temperature (T_0=298.15 K) were applied for calculating all exergy related parameters, as well as physical exergy of a stream of matter:

$$e_j^{\mathrm{PH}} = e_j = \left(h_j - h_0\right) - T_0\left(s_j - s_0\right). \tag{12}$$

The total exergy destruction is sum of partials exergy destructions of the observed heat pump:

$$\dot{E}_{\mathrm{D,tot}} = \Sigma\dot{E}_{\mathrm{D},k} + \Sigma\dot{E}_{\mathrm{D,CD}m}. \tag{13}$$

Very useful parameters in exergy analysis are the component exergy destruction ratio and the system exergy loss ratio, determined with the following equations [18]:

$$y_{\mathrm{D},k} = \frac{\dot{E}_{\mathrm{D},k}}{\dot{E}_{\mathrm{F,tot}}}; \qquad y_{\mathrm{D,CD}m} = \frac{\dot{E}_{\mathrm{D,CD}m}}{\dot{E}_{\mathrm{F,tot}}}; \qquad y_{\mathrm{L,tot}} = \frac{\dot{E}_{\mathrm{L,tot}}}{\dot{E}_{\mathrm{F,tot}}}. \tag{14}$$

Also, the good information for ranking components for improvements is obtained based on the coefficient of the exergy destruction as a ratio between the exergy destruction of component and the exergy destruction of overall system [17]:

$$y_{\mathrm{D},k}^{*} = \frac{\dot{E}_{\mathrm{D},k}}{\dot{E}_{\mathrm{D,tot}}}; \qquad y_{\mathrm{D,CD}m}^{*} = \frac{\dot{E}_{\mathrm{D,CD}m}}{\dot{E}_{\mathrm{D,tot}}}. \tag{15}$$

In the next level, the total value of component exergy destruction can be decomposed in two parts. One of them represents part with real improvement potential (avoidable part) and second represents the part without improvement potential (unavoidable part) as follows:

$$\dot{E}_{\mathrm{D},k} = \dot{E}_{\mathrm{D},k}^{\mathrm{AV}} + \dot{E}_{\mathrm{D},k}^{\mathrm{UN}}; \qquad \dot{E}_{\mathrm{D,CD}m} = \dot{E}_{\mathrm{D,CD}m}^{\mathrm{AV}} + \dot{E}_{\mathrm{D,CD}m}^{\mathrm{UN}}. \tag{16}$$

The unavoidable part determining based on the unavoidable operating conditions, which predefined in table 3 for every component, as such cannot be reached on current technology level. The unavoidable part of component exergy destruction was determined as [19]:

$$\dot{E}_{\mathrm{D},k}^{\mathrm{UN}} = \dot{E}_{\mathrm{P},k}\left(\frac{\dot{E}_{\mathrm{D},k}}{\dot{E}_{\mathrm{P},k}}\right)^{\mathrm{UN}}; \qquad \dot{E}_{\mathrm{D,CD}m}^{\mathrm{UN}} = \dot{E}_{\mathrm{P,CD}m}\left(\frac{\dot{E}_{\mathrm{D,CD}m}}{\dot{E}_{\mathrm{P,CD}m}}\right)^{\mathrm{UN}}, \tag{17}$$

The previous approach allows to define the maximal exergy efficiency for system component, as [20]:

$$\varepsilon_k^{\max} = \frac{1}{1 + \left(\dot{E}_{\mathrm{D},k}/\dot{E}_{\mathrm{P},k}\right)^{\mathrm{UN}}}; \qquad \varepsilon_{\mathrm{CD}m}^{\max} = \frac{1}{1 + \left(\dot{E}_{\mathrm{D,CD}m}/\dot{E}_{\mathrm{P,CD}m}\right)^{\mathrm{UN}}}. \tag{18}$$

4. Results and discussions

In this paper authors presented results for an ASHP with integrated VRV&VRT control techniques. The system has an air-to-refrigerant outdoor unit and thirteen refrigerant-to-air indoor units. The table 3 shown the overview of the main expressions for exergy parameters determination, and conditions for real and unavoidable working for component and whole system. The properties of process fluids are taken from the CoolProp® library [21].

Table 3. The main exergy parameters expressions

Component/ System	**Exergy definition**		**Operation conditions**	
	Fuel	**Product**	**Real**	**Unavoidable**
Compressor	$\dot{W}_{\mathrm{CM}}$	$\dot{E}_2$ - $\dot{E}_1$	$\eta < 0.85$; $Q_{\mathrm{L}} \neq 0$	$\eta = 0.95$; $Q_{\mathrm{L}} \approx 0$
Condensers	$\dot{W}_{\mathrm{CD}\boldsymbol{m}}$ + ($\dot{E}_{2,m}$ - $\dot{E}_{3,m}$)	$\dot{E}_{\mathrm{au,e},m}$ - $\dot{E}_{\mathrm{au,i},m}$	$\Delta p' = 0$; $\Delta p'' \neq 0$; $Q_{\mathrm{L}} \neq 0$	$\Delta p' = 0$; $\Delta p'' \approx 0$; $Q_{\mathrm{L}} \approx 0$
Expansion valve	$\dot{E}_3$	$\dot{E}_4$	h = *const.*; $Q_{\mathrm{L}} \neq 0$	h = *const.*; $Q_{\mathrm{L}} \approx 0$
Evaporator	$\dot{W}_{\mathrm{EV}}$ + ($\dot{E}_{\mathrm{a0,e}}$ - $\dot{E}_{\mathrm{a0,i}}$)	$\dot{E}_4$ - $\dot{E}_1$	$\Delta p' = \Delta p'' = 0$; $Q_{\mathrm{L}} \neq 0$	$\Delta p' = \Delta p'' = 0$; $Q_{\mathrm{L}} \approx 0$
ASHP	$\dot{W}_{\mathrm{tot}}$ + ($\dot{E}_{\mathrm{a0,e}}$ - $\dot{E}_{\mathrm{a0,i}}$)	$\Sigma\dot{E}_{\mathrm{P,CD}\boldsymbol{m}}$		

For the main process fluids, the profiles of temperature and pressure in the working conditions, as well as the target profiles, are presented in figure 3. In the starting period the temperature and pressure of condensation increases until the achievements of the stationary regime. At the middle part and at the end of the observed period, were recorded non-stationary regimes, which registered a sudden drop of parameters. The reason is entering in the defrosting regime. In the middle zone presented profiles of inside temperature in all spaces (13 offices) as well as the set value of inside temperature for all offices ($t_{\mathrm{u,tar}}$ = 26.0°C). Only in one office (No. 3) the temperature was dropping because the indoor unit was not in working order, but in the other offices the temperature was maintained around the set value (from 23.1°C to 26.0°C). On the same diagram (figure 3) in the lower zone shows the current values of evaporation and outdoor temperature, and the target values od evaporation temperature and pressure. The target evaporation temperature is lower than outdoor temperature, ranged from 0.1°C to 1.1°C. This average value has been 6.24°C below the set values.

The outdoor temperature during the observed period ranged from 14.0°C (max) to of 2.3°C (min), Table 4 and Figures 3, 4 and 5. The heating needs increased when the outdoor temperature decreased. However, due to the significant building envelope inertia, this growth is very small (from 6.2 kW to 6.5 kW).

Having in mind very low value of standard deviation (0.1 kW, table 4) many measured data are concentrate near the average value (6.4 kW, table 4), figure 4.

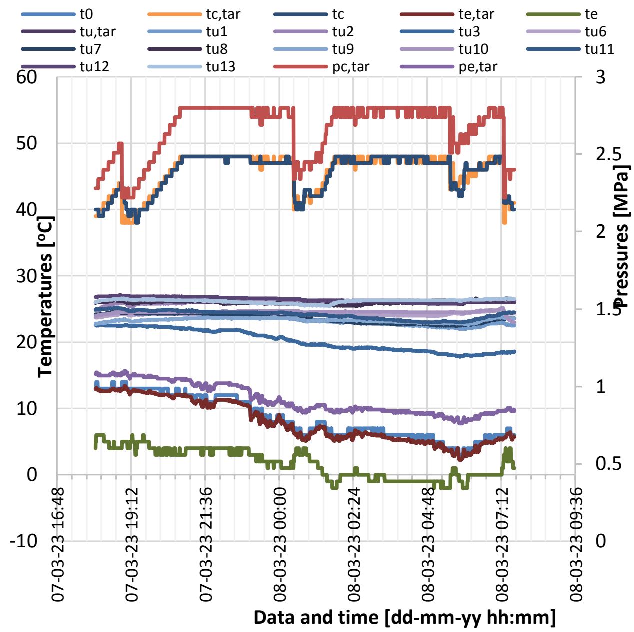

Figure 3. Profiles of parameters during the time

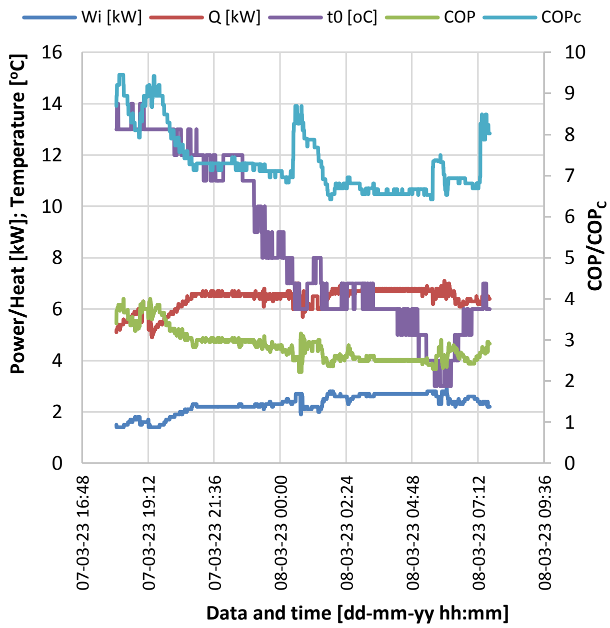

Figure 4. Main characteristics during the time

Considering that it was analyzed the air-source heat pump, lower amount of energy comes from the environment when the outside air temperature drops. In that case, more electricity must be taken from the public power network in first line for compressor operation (from 1.9 kW to 3.0 kW). The temperature lift increases consequently (from 30.3°C to 49.4°C). Also, Coefficient of performance decreased from 3.3 to 2.1, Figure 4 and Table 4, with value of standard deviation of 0.3.

Accordance with equation (4) the profile of COPc for ideal Carnot cycle presents on figures 4 and 5. Based on statistical analysis it was concluded that the mean values are relevant for further analysis.

The ASHP exergy efficiency decreases when the exergy of fuel increases, Figure 6. The dominant effect comes from evaporator exergy efficiency. From the other hand, the influence which comes from other components is opposite. The middle value of exergy efficiency for ASHP is 22.4% (ranged from 14.9% to 32.1% with standard deviation range of 3.8 kW), table 4. When the heat pump exergy of fuel increases the exergy efficiency of condensers and compressor are declining, figure 6.

Table 4. The statistical quantities of main parameters

Statistical quantities	**The main parameters**									
	t_0	Δt_{lift}	$\dot{W}_{tot}$	$\dot{Q}_{tot}$	$COP_{\mathbf{tot}}$	$\dot{E}_{F,tot}$	$\dot{E}_{P,tot}$	$\dot{E}_{D,tot}$	$\dot{E}_{L,tot}$	ε_{tot}
	[°C]	[°C]	[kW]	[kW]	[-]	[kW]	[kW]	[kW]	[kW]	[%]
MAX	14.0	49.4	3.0	6.5	3.3	2.99	0.8	1.4	1.2	32.1
MIN	2.3	30.3	1.9	6.2	2.1	2.03	0.4	0.8	0.4	14.9
AVR	9.0	43.4	2.7	6.4	2.4	2.68	0.6	1.2	0.9	22.4
MED	8.0	43.7	2.7	6.4	2.4	2.71	0.5	1.3	0.9	21.9
STD	3.0	4.4	0.3	0.1	0.3	0.26	0.1	0.1	0.1	3.8

The heat pump had the average value of exergy efficiency 22.35%, figure 7. The main impact on her reducing has an ireversibillities in compressor with value of exergy destruction coefficient of 17.39%. The negative impacts from evaporator and expansion valve are 7.90% and 4.32%, respectively. The negative impact of every condenser range from 0.72% to 2.0%. The exergy loss with value of its coefficient of

33.55% has the biggest impact on the ASHP exergy efficiency reduction, figure 7. It should be noted that the indoor unit in office number three (which is out of order) has a negative impact also, given that the system requires a minimum technological flow through all indoor units of 15%.

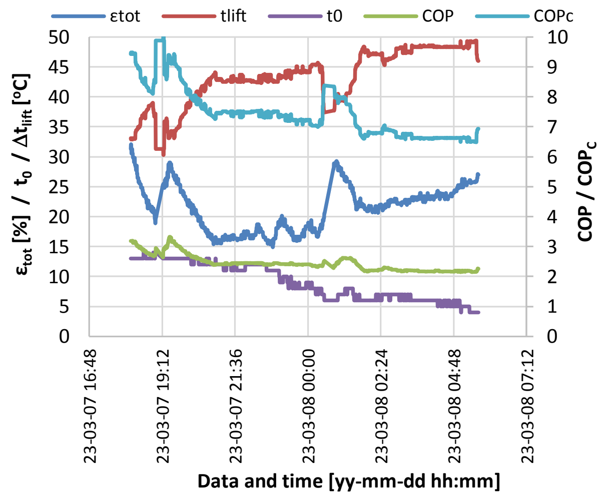

Figure 5. Energy/exergy parameters during the time

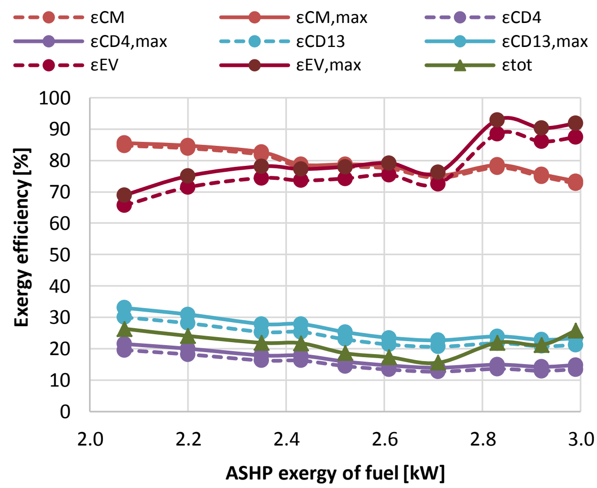

Figure 6. Exergy efficiency vs exergy of fuel

Accordance with equation (15) the total exergy destruction coefficients show on figure 8. The compressor has the largest share (37% or 0.37). Evaporator participates with share of 17% (0.17) and share of the expansion valve is 10% (0.10). The smallest shares have the condensers, whose shares ranges from 2% to 5%, figure 8.

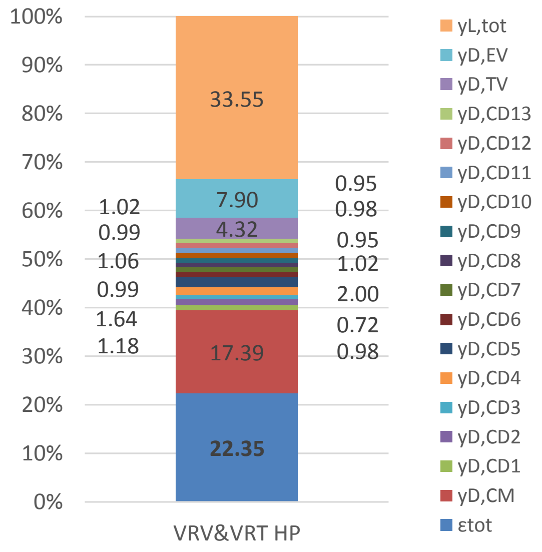

Figure 7. Exergy efficiency & reducing impacts

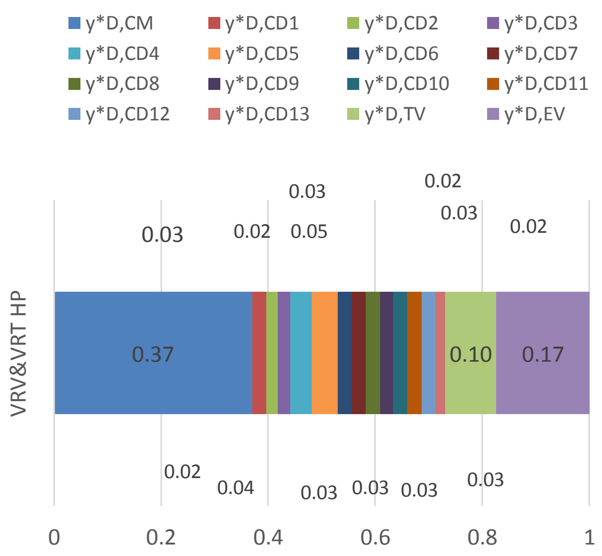

Figure 8. The total exergy destruction coefficients

Accordance with equations (10) and (16) exergy of fuel and destroyed exergy for every component of ASHP decomposed additionally. From 2.01 kW as a total exergy of fuel for compressor, the useful exergy is 70% (exergy of product) and 30% was destroyed due internal irreversibilies. Furter, from 0.60 kW as a total exergy destruction, 27% can be avoided and 73% cannot be avoided, figure 9a.

From 0.07 kW as a total exergy of fuel for condenser No. 13, the useful exergy is 69% (exergy of product) and 31% was destroyed due internal irreversibilies. Furter, from 0.02 kW as a total exergy destruction, 14% can be avoided and 86% cannot be avoided, figure 9b. The condenser number 13 (CD13) was chosen arbitrarily since the influence of almost all indoor units is approximately equal.

From 0.91 kW as a total exergy of fuel for evaporator, the useful exergy is 78% (exergy of product) and 22% was destroyed due internal irreversibilies. Furter, from 0.20 kW as a total exergy destruction, 20% can be avoided and 80% cannot be avoided, figure 9c.

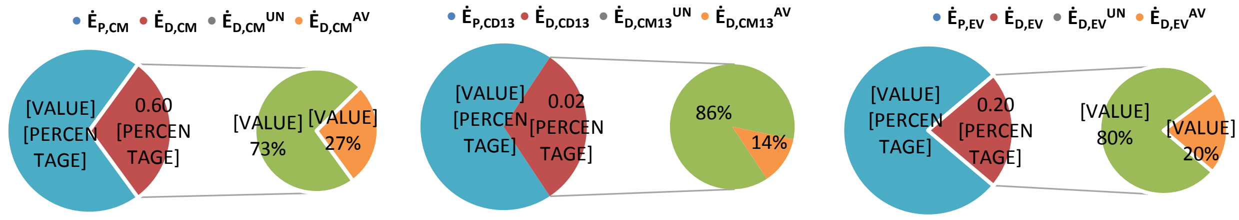

a) Speed control compressor | *b) Indoor heat exchanger No.13* | *c) Outdoor heat exchanger*

Figure 9. Decomposition of component destroyed exergy

5. Conclusions

The performance assessment of an ASHP with VRV&VRT technologies based first and second laws gives follows conclusions:

- From energy-based aspect (the energy quantity aspect) the heat pump operated with good value of performance ($\overline{\mathrm{COP}}_{\mathrm{tot}} = 2.4$),
- From exergy-based aspect (the energy quality aspect) the heat pump operated with very small value of exergy efficiency ($\bar{\varepsilon}_{\mathrm{tot}} = 22.4\%$). The dominant negative impact has internal irreversibilities in the compressor and total exergy loss,
- The evaporation temperature was much lower on average 6.24°C below the set values.

The biggest impact with 17.4% on reducing exergy efficiency of observed ASHP has internal ireversibilities in the speed control compressor. Destroyed work in other main components (evaporator, expansion valve and all condensers) generated cumulative negative impact of 26.7%. Additionally, the exergy losses reduced exergy efficiency by 33.5%.

If the applied the best techniques, the 27% of destroyed useful work in compressor can be avoided, but the bigger part (73%) is unavoidable. In the same way only 20% of destroyed useful work in the evaporator can be avoided. In accordance with the above for improving the ASHP efficiency during heating operation it is important to reduce the internal ireversibilities in the compressor, evaporator and all condensers, and decrease the exergy losses. Both the energy-based and the exergy-based analyses indicate that the temperature difference should be as low as possible from condensing to evaporating.

An additional suggestion is to find a technical solution to completely switch-off the flow rate through the indoor units when they are not in operation.

Acknowledgments

This research was financially supported by the Ministry of Science, Technological Development and Innovation of the Republic of Serbia (Contract No. 451-03-65/2024-03).

Nomenclature

e	- specific exergy (kJkg^{-1})	EV	- evaporator
$\dot{E}$	- exergy flow rate (kW)	F	- fuel
h	- specific enthalpy (kJkg^{-1})	*i*	- current measure, inlet stream
$\dot{m}$	- mass flow rate (kgs^{-1})	*j*	- current stream
p	- pressure (bar)	*k*	- component (except condensers)
$\dot{Q}$	- heat transfer rate (kW)	lift	- from condensation to evaporation

s	- specific entropy ($kJkg^{-1}K^{-1}$)
$\dot{S}$	- entropy rate (WK^{-1})
t	- temperature (°C)
T	- absolute temperature (K)
$\dot{W}$	- power rate, work rate (kW)
X	- current variable
y	- exergy ratio

Greek symbols

Δ	- difference
ε	- exergy efficiency
μ	- median
σ	- standard deviation

Subscripts

a	- air (inside or outside)
c	- condensation
C	- Carnot
CD	- condenser
CM	- compressor
cv	- control volume
D	- destruction
e	- evaporation, outlet stream
L	- loss
m	- number of IU (m=1÷13)
max	- maximal
min	- minimal
N	- total number of measures
P	- product
q	- heat transfer
tar	- setup value
EV	- expansion valve
tot	- whole system (ASHP)
X	- current variable
u	- inside
0	- environment, outdoor

Superscripts

AV	- avoidable
max	- maximal
PH	- physical
UN	- unavoidable
*	- total
$\bar{}$	- arithmetic average

References

[1] ***, https://iea.blob.core.windows.net/assets/d718c314-c916-47c9-a368-9f8bb38fd9d0/CleanEnergyMarketMonitorMarch2024.pdf

[2] ***, https://www.ehpa.org/market-data/

[3] ***, https://www.globenewswire.com/en/news-release/2022/12/08/2570652/0/en/Heat-Pump-Market-Size-is-Expected-to-Surpass-USD-139-4-Bn-By-2030.html

[4] ***, https://www.apex-surveys.co.uk/post/the-invention-of-air-source-heat-pumps-a-sustainable-heating-revolution

[5] Sharma C., Raustad R., Compare energy use in variable refrigerant flow heat pumps field demonstration and computer model, ASHRE Annual Conference 2013.

[6] Zhang R., Sun K., Hong T., Yura Y., Hinokuma R., A novel Variable Refrigerant Flow (VRF) heat recovery system model: Development and validation, *Energy and Buildings, 168* (2018), pp. 399-412.

[7] Aynur T.N., Hwang Y.H., Radermacher R., Field performance measurements of a heat pump desiccant unit in dehumidification mode, *Energy and Buildings, 40* (2008), pp. 2141-2147.

[8] Hong T., Sun K., Zhang R., Hinokuma R., Kasahara S., Yura., Development and validation of a new variable refrigerant flow system model in EnergyPlus, *Energy and Buildings, 117* (2016) pp. 399-411.

[9] Hyeon L.J., Song S., Song Y., Verification of refrigerant evaporating temperature control effect in VRF systems in actual buildings, *Energy and Buildings, 250 (111295)* (2021) pp. 1-12.

[10] Pallis P., Braimakis K., Roumpedakis T., Varvagiannis E., Karellas S., Doulos L., Katsaros M., Vourliotis P., Energy and economic performance assessment of efficiency measures in zero-energy office buildings in Greece, *Energy & Environment*, 206(108378) (2021) pp. 1-19.

[11] Kwon L., Lee H., Hwang Y., Radermacher R., Kim B., Experimental investigation of multifunctional VRF system in heating and shoulder seasons, *Applied Thermal Engineering, 66* (2014) pp. 355-364.

[12] Zhaoa D., Zhanga X., Zhong M., Variable evaporating temperature control strategy for VRV system under part load conditions in cooling mode, *Energy and Buildings, 91* (2015) pp. 180-186.

[13] Aynur N. T., Variable refrigerant flow systems: A review, *Energy and Buildings, 42* (2010) pp. 1106-1112.

[14] ***, https://www.daikin.rs/sr_rs/products/product.html/

[15] Ristić B., *Metrology, Flow-technical measurements (in Serbian)*, Prosveta, Niš, 1981.

[16] Cuhla O., Gunerhan H., Biyik E., Ekren O., Hepbasli A., Heat exchanger applications in wastewater source heat pumps for buildings: A key review, *Energy and Buildings, 104* (2015) pp. 215-232.

[17] Mergenthaler P., Schinkel A.P., Tsatsaronis G., Application of exergoeconomic, exergoenvironmental, and advanced exergy analysis to Carbon Black production, *Energy, 137* (2017) pp. 898-907.

[18] Bejan A., Tsatsaronis G., *Moran M., Thermal design and optimization*, John Wiley & Sons, Inc., New York, 1996.

[19] Ebrahimi M., Carriveau R., Ting D.S.-K., McGillis A., Conventional and advanced exergy analysis of a grid connected underwater compressed air energy storage facility, *Applied Energy, 242* (2019) pp. 1198-1208.

[20] Kelly S., *Energy system improvement based on endogenous and exogenous exergy destruction*, PhD Thesis, TU Berlin, 2008.

[21] ***, http://www.coolprop.org/index.html

Submitted : 23.12.2024.

Revised: 28.01.2025

Accepted: 31.01.2025.